JOURNAL OF COMPUTATIONAL PHYSICS 23, 242–262 (1977)

A Multistep Technique for the Numerical Solution of a Two-Dimensional Vlasov Equation

M. M. SHOUCRI AND R. R. J. GAGNÉ

Department of Electrical Engineering, Laval University, Quebec City, Canada

Received December 19, 1975; revised March 15, 1975

This work describes a multistep technique for the numerical solution of a two-dimensional Vlasov equation. The equation is first transformed, with respect to the two velocity variables v_x and v_y, by expanding the distribution function $f(x, y, v_x, v_y, t)$ in terms of Hermite polynomials. The transformed equation is then integrated at each time step first in the x direction, and next in the y direction and vice versa. The numerical scheme is tested by studying the two-dimensional free streaming case and the linear Landau damping. The results show very good agreement with the theory.

1. INTRODUCTION

This paper discusses numerical methods and techniques for the solution of a two-dimensional Vlasov equation. We are dealing essentially with the dimensionless equation

$$\frac{\partial f}{\partial t} + v_x \frac{\partial f}{\partial x} + v_y \frac{\partial f}{\partial y} + E_x(x, y, t) \frac{\partial f}{\partial v_x} + E_y(x, y, t) \frac{\partial f}{\partial v_y} = 0 \tag{1}$$

supplemented with the Poisson equation

$$(\partial E_x/\partial x) + (\partial E_y/\partial y) = \iint_{-\infty}^{\infty} f \, dv_x \, dv_y - 1. \tag{2}$$

The units of time, velocity, and space used in Eqs. (1) and (2) are the inverse plasma frequency, $\omega_p^{-1} = (4\pi n_0 e^2/m)^{-1/2}$, the thermal velocity $v_t = (KT/m)^{1/2}$, and the Debye length $\lambda_D = (KT/4\pi n_0 e^2)^{1/2}$. The other symbols have their conventional meaning.

In recent years, numerical techniques have been successfully applied to the study of the nonlinear solution of the one-dimensional Vlasov equation [1–10]. The difficulty in the numerical solution of this equation is that the distribution function f tends to develop filamentation in phase space as time progresses [5].

ISSN 0021-9991

When a difference scheme is used for the velocity derivative term in the solution of Eq. (1), this filamentation requires smaller steps for the difference scheme and, consequently, an ever increasing computational effort for large times. Among the methods developed to overcome this difficulty, the use of velocity transform methods for the numerical solution of the one-dimensional Vlasov equation has been discussed and reviewed by Armstrong *et al.* [1] and Joyce *et al.* [2]. The expansion of the distribution function in velocity space in terms of orthogonal polynomials, namely the Hermite polynomials, has been particularly studied by Grant and Feix [3], Armstrong [4], and Knorr [5]. The choice of the Hermite polynomials has been essentially dictated by the fact that no other classical polynomials possess such a simple expression for their derivatives.

When transform methods are used to solve the one-dimensional Vlasov equation, a representation in spatial Fourier modes can be used as in [3, 4]. In this case the product $E_x(x, t)(\partial f(x, v_x, t)/\partial v_x)$ is transformed into convolution sums, thus increasing the computational effort. This drawback has been realized by Nuehrenberg [6] and Knorr [5], who transformed the one-dimensional Vlasov equation in velocity space, and solved the resulting equation using an appropriate difference scheme in configuration space. The velocity transformation used by Knorr [5] consisted in expanding the distribution function in velocity space in terms of Hermite polynomials; this resulted in a hyperbolic equation in configuration space which was solved using a two-level leapfrog scheme, initialized by using a two-level Lax–Wendroff scheme. These schemes have also been successfully applied by Shoucri and Knorr [7] in connection with the Chebyshev representation of the Vlasov equation, and, more recently, by Shoucri and Gagné [8] (a detailed analysis of this scheme has been given in [5]). It is the purpose of the present work to extend the methods and the techniques previously developed for the study of the one-dimensional problem, particularly in [5, 7, 8], to the solution of the two-dimensional Vlasov equation (the set of Eqs. (1)–(2)). First, the equation will be transformed by expanding the distribution function $f(x, y, v_x, v_y, t)$ in velocity space in terms of Hermite polynomials, then the resulting 2-D hyperbolic differential equation will be solved in configuration space; this is effected by applying a multistep technique [11] which consists of splitting up the two-dimensional equation and integrating it successively in the x and y direction and vice versa, using the leapfrog scheme previously applied to the one-dimensional case. The numerical scheme is tested by studying the free streaming case and also the linear Landau damping. Preliminary results of these studies have been reported in [12].

Section 2 will describe the Hermite representation of the two-dimensional Vlasov equation. In Section 3, we study the eigenvalue theory of the truncated system of equations in two dimensions; a discussion of the same problem for an infinite matrix, together with the evaluation of the recurrence time for a two-dimensional

truncated matrix, is given in the Appendix. In Section 4, we discuss the formal addition of damping to the Vlasov equation, this addition being made to render the solution of the truncated system more similar to the one of the infinite system. Section 5 presents the finite difference scheme which is used for solving, in configuration space, the two-dimensional Hermite representation of the Vlasov equation derived in Section 2. This scheme is a two-level scheme, and needs to be initialized properly; this initialization is discussed in Section 6. Section 7 presents the numerical results and a comparison is made with available analytical results. Finally, Section 8 presents the conclusions.

2. Representation of the Two-Dimensional Vlasov Equation in Terms of Hermite Polynomials

We expand the velocity dependence v_x and v_y, of the distribution function f, using the series of Hermite polynomials $H_{ev}(v_x)$ and $H_{e\mu}(v_y)$

$$f(x, y, v_x, v_y, t) = (1/2\pi) \sum_{\nu=0}^{\infty} \sum_{\mu=0}^{\infty} h_\nu h_\mu b_{\nu,\mu}(x, y, t)\, H_{ev}(v_x)\, H_{e\mu}(v_y) \exp(-\tfrac{1}{2}v_x^2 - \tfrac{1}{2}v_y^2). \tag{3}$$

The constants h_ν and h_μ are arbitrary and will be adjusted as in [5] for a maximum of numerical convenience. When the series in Eq. (3) is inserted in Eq. (1), and coefficients for the Hermite polynomials are collected, one obtains the infinite system of differential equations

$$\frac{\partial b_{\nu,\mu}}{\partial t} + \frac{h_{\nu-1}}{h_\nu}\frac{\partial b_{\nu-1,\mu}}{\partial x} + \frac{h_{\nu+1}}{h_\nu}(\nu+1)\frac{\partial b_{\nu+1,\mu}}{\partial x} - \frac{h_{\nu-1}}{h_\nu} E_x b_{\nu-1,\mu} + \frac{h_{\mu-1}}{h_\mu}\frac{\partial b_{\nu,\mu-1}}{\partial y} + \frac{h_{\mu+1}}{h_\mu}(\mu+1)\frac{\partial b_{\nu,\mu+1}}{\partial y} - \frac{h_{\mu-1}}{h_\mu} E_y b_{\nu,\mu-1} = 0. \tag{4}$$

We adjust the h_ν coefficients, following the same method as in [5], in such a way as to make the two coefficients $h_{\nu-1}/h_\nu$ and $h_{\nu+1}(\nu+1)/h_\nu$ equal; the h_μ coefficients are adjusted in the same way. As a result, Eq. (4) will contain only the coefficients ρ_ν and ρ_μ defined by

$$\rho_\nu = h_{\nu-1}/h_\nu . \tag{5}$$

The recursion relation

$$\rho_\nu \rho_{\nu+1} = \nu + 1 \tag{6}$$

holds for ρ_ν and a similar relation also applies for the coefficients ρ_μ. Equation (4) thus becomes

$$\dot{b}_{\nu,\mu} + \rho_\nu[(\partial/\partial x)(b_{\nu-1,\mu} + b_{\nu+1,\mu}) - E_x(x, y, t)\, b_{\nu-1,\mu}] + \rho_\mu[(\partial/\partial y)(b_{\nu,\mu-1} + b_{\nu,\mu+1}) - E_y(x, y, t)\, b_{\nu,\mu-1}] = 0. \tag{7}$$

The choice of ρ_0 is arbitrary. We follow [5] and choose $\rho_0 = 1$. Similarly we choose $h_0 = 1$, from which it follows that $h_1 = 1$, $h_2 = \frac{1}{2}$, etc.

For convenience, the distribution function is sometimes split into an homogeneous part and a perturbation part, in a way similar to that followed when linearizing the Vlasov equation. We thus write

$$f(x, y, v_x, v_y, t) = f_0(v_x, v_y) + f_1(x, y, v_x, v_y, t) \tag{8}$$

where $f_1(x, y, v_x, v_y, t)$ is expanded using the series in Eq. (5). If we choose $f_0(v_x, v_y)$ to be a Maxwellian distribution

$$f_0(v_x, v_y) = (1/2\pi) \exp(-\tfrac{1}{2}v_x^2 - v_y^2) \tag{9}$$

we then obtain, in lieu of Eq. (7),

$$\begin{aligned} \dot{b}_{\nu,\mu} &+ \rho_\nu[(\partial/\partial x)(b_{\nu-1,\mu} + b_{\nu+1,\mu}) - E_x b_{\nu-1,\mu}] - E_x \delta_{1\nu}\delta_{0\mu} \\ &+ \rho_\mu[(\partial/\partial y)(b_{\nu,\mu-1} + b_{\nu,\mu+1}) - E_y b_{\nu,\mu-1}] - E_y \delta_{0\nu}\delta_{1\mu} = 0 \end{aligned} \tag{10}$$

where δ is the Kronecker symbol. The neglect of the terms $E_x b_{\nu-1,\mu}$ and $E_y b_{\nu,\mu-1}$ in Eq. (10) will correspond to the exact linearization of the Vlasov equation.

The system in Eqs. (7) and (10) is infinite, since the summation in Eq. (3) extends, for ν and μ, up to infinity. In numerical calculations however, a computer can handle finite systems only and one is obliged to truncate the infinite system in Eq. (7) or Eq. (10) at, say, $\nu = N_x$ and $\mu = N_y$, by setting arbitrarily

$$b_{N_x,N_y}(x, y, t) = 0. \tag{11}$$

The substitution from Eq. (11) changes drastically the nature of the system in Eqs. (7) and (10), since one is replacing the continuous eigenvalue spectrum of these equations, by the discrete number of eigenvalues of the truncated system. This results in a truncation instability (or recurrence effect) which has been extensively discussed for the one-dimensional problem [2, 5, 13].

Similar effects also appear in the two-dimensional case, and, to obtain a clear comprehension of these effects, it is well worthwhile to go through the eigenvalue theory of the two-dimensional system.

3. The Eigenvalue Theory

We set the electric field in Eq. (1) equal to zero for the moment and consider the "free streaming" case

$$(\partial f/\partial t) + v_x(\partial f/\partial x) + v_y(\partial f/\partial y) = 0. \tag{12}$$

The solution of Eq. (12) is clearly

$$f(x, y, v_x, v_y, t) = f(x - v_x t, y - v_y t, v_x, v_y, 0). \tag{13}$$

Substituting from Eq. (3) in Eq. (12), we get

$$\dot{b}_{\nu,\mu} + \rho_\nu(\partial/\partial x)(b_{\nu-1,\mu} + b_{\nu+1,\mu}) + \rho_\mu(\partial/\partial y)(b_{\nu,\mu-1} + b_{\nu,\mu+1}) = 0. \tag{14}$$

When the infinite system in the previous equation is truncated at, say, $\nu = N_x$ and $\mu = N_y$, by setting $b_{N_x,N_y}(x, y, t) = 0$, the continuous eigenvalue spectrum of this sytem is replaced by the set of discrete finite eigenvalues of the truncated system. To determine these eigenvalues and the corresponding eigensolution, we try the ansatz

$$b_{\nu,\mu}(x, y, t) = (-i)^\nu(-i)^\mu b_{\nu,\mu} \exp(ik_x x + ik_y y + \Lambda t). \tag{15}$$

From Eq. (14), we obtain

$$\Lambda b_{\nu,\mu} + k_x\rho_\nu(-b_{\nu-1,\mu} + b_{\nu+1,\mu}) + k_y\rho_\mu(-b_{\nu,\mu-1} + b_{\nu,\mu+1}) = 0. \tag{16}$$

We next substitute in Eq. (16) by

$$b_{\nu,\mu} = \zeta_\nu\zeta_\nu H_\nu H_\mu \tag{17}$$

and choose the parameter ζ_ν such that

$$(\zeta_\nu/\zeta_{\nu+1}) = i\rho_\nu . \tag{18}$$

We also choose $\zeta_0 = 1$; in this case one can easily verify that $\zeta_\nu h_\nu = (-i)^\nu/\nu!$. We make a similar choice for the ζ_μ, which results in a similar relation for $\zeta_\mu h_\mu$. With the help of Eq. (6), we get from Eqs. (16), (18)

$$\Lambda H_\nu H_\mu + ik_x(-\nu H_{\nu-1}H_\mu - H_{\nu+1}H_\mu) + ik_y(-\mu H_\nu H_{\nu-1} - H_\nu H_{\mu+1}) = 0. \tag{19}$$

We assume that the value of Λ can be written in the form

$$\Lambda = i\omega_x + i\omega_y , \tag{20}$$

in which case Eq. (19) is rewritten

$$\omega_x + k_x(-\nu(H_{\nu-1}/H_\nu) - (H_{\nu+1}/H_\nu)) + \omega_y + k_y(-\mu(H_{\mu-1}/H_\mu) - (H_{\mu+1}/H_\mu)) = 0. \tag{21}$$

The reason Λ was split up into two parts in Eq. (20) is that, as a result, Eq. (21) can be split up into two symmetric parts which are just the recurrence relation for the Hermite polynomials. Hence a solution for Eq. (21) can be found if H_ν and H_μ are expressed in terms of Hermite polynomials

$$H_\nu = H_{e\nu}(\omega_x/k_x), \tag{22}$$

$$H_\mu = H_{e\mu}(\omega_y/k_y). \tag{23}$$

For the infinite system in Eq. (14), the eigenvalue spectrum is continuous. The time evolution of the distribution function f in this case is discussed in the Appendix.

The system is finite if we require that Eq. (11) hold for $\nu = N_x$ and $\mu = N_y$, i.e., if ω_x/k_x and ω_y/k_y are such that

$$H_{eN_x}(\omega_x/k_x) = 0, \tag{24}$$

$$H_{eN_y}(\omega_y/k_y) = 0, \tag{25}$$

or, equivalently, if

$$\omega_x = k_x Z_\alpha^{N_x}, \qquad \alpha = 1, 2, \ldots, N_x, \tag{26}$$

$$\omega_y = k_y Z_\beta^{N_y}, \qquad \beta = 1, 2, \ldots, N_y, \tag{27}$$

where $Z_\alpha^{N_x}$ and $Z_\beta^{N_y}$ are the αth and βth root of the Hermite polynomials H_{eN_x} and H_{eN_y}, respectively. Substituting the previous results into Eq. (3), we get for the free streaming case

$$\begin{aligned} f(x, y, v_x, v_y, t) = \frac{1}{2\pi} \sum_{\nu=0}^{N_x} \sum_{\mu=0}^{N_y} \sum_{\alpha=0}^{N_x} \sum_{\beta=0}^{N_y} \frac{A_{\alpha,\beta}}{\nu!\mu!} H_{e\nu}(Z_\alpha^{N_x}) H_{e\mu}(Z_\beta^{N_y}) \\ \cdot H_{e\nu}(v_x) H_{e\mu}(v_y) \exp(-\tfrac{1}{2}v_x^2 - \tfrac{1}{2}v_y^2) \exp[(ik_x x + ik_y y) \\ + i(k_x Z_\alpha^{N_x} + k_y Z_\beta^{N_y})]\, t, \end{aligned} \tag{28}$$

where the constants $A_{\alpha,\beta}$ are to be determined from the initial conditions. Equation (28) indicates that the individual modes are periodic functions of time resulting in an almost periodic distribution function (an estimation of the recurrence time, for an initially Maxwellian distribution, is given in the Appendix), a behavior which is totally different from that for the continuous spectrum which shows the individual modes decaying to zero as time elapses, while the perturbation is transfered to modes of ever increasing order (Eq. (A.7)).

4. The Addition of Damping

In order to make the solution for the truncated system similar to the one for the infinite system, a method was suggested in [2] which consists of formally adding an imaginary part to the eigenvalues calculated in Eqs. (26), (27). This corresponds physically to the presence of dissipative terms on the right-hand side of Eq. (14), such as a "collision term," for example. A study of this term for the one-dimensional Hermite representation of the Vlasov equation has been given by Knorr

and Shoucri [14], and the results can be readily generalized for the two-dimensional case. The damping operator used in the present calculations is of the form

$$\lambda C(v)^{2r+1}f + \eta\nabla^2 C(v)^{2r+1}f, \tag{29}$$

where $C(v)$ is the Fokker–Planck operator

$$C(v) \equiv (\partial/\partial v_x)(v_x + (\partial/\partial v_x) + (\partial/\partial v_y)(v_y + (\partial/\partial v_y) \tag{30}$$

and

$$\nabla^2 \equiv (\partial^2/\partial x^2) + (\partial^2/\partial y^2), \tag{31}$$

λ and η are constants, and r is an integer. The use of this operator corresponds to formally adding to the right-hand side of Eq. (14) a damping term given by

$$-(\nu + \mu)^{2r+1}(\lambda + \eta\nabla^2)\, b_{\nu,\mu}(x, y, t). \tag{32}$$

The term with λ effects a selective damping of the coefficients with large values of ν or μ; this corresponds to a smoothing of the distribution function if the ripples in velocity space exceed a certain steepness. The second term with η adds to the previous smoothing effect by causing a selective damping of the Fourier components having the highest wavenumbers (hence the lowest recurrence time, since, as shown in the Appendix, the recurrence time is given by

$$T_R = 2(N_x + N_y)^{1/2}(k_x^2 + k_y^2)^{-1/2}).$$

5. The Finite Difference Scheme

The system in Eq. (10) is hyperbolic, and, rather than solving it as whole for each time step, we split up the equation and use a multistep technique [11] whereby the equation is integrated first in the x direction and next in the y direction (or vice versa). More explicitly, we solve for the first half time-step:

$$b_{\nu,\mu} + \rho_\nu[(\partial/\partial x)(b_{\nu-1,\mu} + b_{\nu+1,\mu}) - E_x b_{\nu-1,\mu}] - E_x\delta_{1\nu}\delta_{0\mu} = 0 \tag{33}$$

(together with Poisson's equation), and then, for the second half time-step, we solve the equation

$$b_{\nu,\mu} + \rho_\mu[(\partial/\partial y)(b_{\nu,\mu-1} + b_{\nu,\mu+1}) - E_y b_{\nu,\mu-1}] - E_y\delta_{0\nu}\delta_{1\mu} = 0 \tag{34}$$

(together with Poisson equation). Whether Eq. (34) is integrated before Eq. (33) is arbitrary. Gourlay and Morris [15] suggested a procedure where the integrated value for a time-step is calculated by averaging the two values obtained by integrating the same initial value twice, first in the x to y direction and next in the y to x direction. The procedure however could be very time consuming since the integration has to be repeated twice for each time step. Instead, we use the

following, more economical, method: at a first time-step Eq. (7) is integrated in the x direction then in the y direction, then we alternate at the following time step and integrate the equation first in the y direction and then in the x direction, and we keep alternating directions at successive time-steps. The results obtained by this method have been compared, for the free streaming case, to those obtained using the previously described method by Gourlay and Morris [15], and were found to be identical.

Equations (33) and (34) are hyperbolic equations and are solved numerically using a leapfrog scheme which was used for the one-dimensional problem by Knorr [5], Shoucri and Knorr [7], and Shoucri and Gagné [8].

The leapfrog scheme is two-level, and if we integrate Eq. (33) first, the difference scheme takes the form (note that $\rho_1 = 1$)

$$\begin{aligned} b_{\nu,\mu}^{n+1}(j_x, j_y) = b_{\nu,\mu}^{n}(j_x, j_y) - \rho_\nu(\Delta t/2\,\Delta x)\{&b_{\nu-1,\mu}^{n+(1/2)}(j_x + \tfrac{1}{2}, j_y + \tfrac{1}{2}) \\ &+ b_{\nu-1,\mu}^{n+(1/2)}(j_x + \tfrac{1}{2}, j_y - \tfrac{1}{2}) - b_{\nu-1,\mu}^{n+(1/2)}(j_x - \tfrac{1}{2}, j_y + \tfrac{1}{2}) \\ &- b_{\nu-1,\mu}^{n+(1/2)}(j_x - \tfrac{1}{2}, j_y - \tfrac{1}{2}) + b_{\nu+1,\mu}^{n+(1/2)}(j_x + \tfrac{1}{2}, j_y + \tfrac{1}{2}) \\ &+ b_{\nu+1,\mu}^{n+(1/2)}(j_x + \tfrac{1}{2}, j_y - \tfrac{1}{2}) - b_{\nu+1,\mu}^{n+(1/2)}(j_x - \tfrac{1}{2}, j_y + \tfrac{1}{2}) \\ &- b_{\nu+1,\mu}^{n+(1/2)}(j_x - \tfrac{1}{2}, j_y - \tfrac{1}{2})\} \\ &+ \rho_\nu\,\Delta t\, E_x^{n+(1/2)}(j_x, j_y)[\tilde{b}_{\nu-1,\mu}^{n+(1/2)}(j_x, j_y) + \delta_{1\nu}\delta_{0\mu}], \end{aligned} \tag{35}$$

$$\begin{aligned} b_{\nu,\mu}^{n+(3/2)}(j_x + \tfrac{1}{2}, j_y + \tfrac{1}{2}) \\ = b_{\nu,\mu}^{n+(1/2)}(j_x + \tfrac{1}{2}, j_y + \tfrac{1}{2}) - \rho_\nu(\Delta t/2\,\Delta x)\{&b_{\nu-1,\mu}^{n+1}(j_x + 1, j_y + 1) \\ &+ b_{\nu-1,\mu}^{n+1}(j_x + 1, j_y) - b_{\nu-1,\mu}^{n+1}(j_x, j_y + 1) - b_{\nu-1,\mu}^{n+1}(j_x, j_y) \\ &+ b_{\nu+1,\mu}^{n+1}(j_x + 1, j_y + 1) + b_{\nu+1,\mu}^{n+1}(j_x + 1, j_y) - b_{\nu+1,\mu}^{n+1}(j_x, j_y + 1) \\ &- b_{\nu+1,\mu}^{n+1}(j_x, j_y)\} + \rho_\nu\,\Delta t\, E_x^{n+1}(j_x + \tfrac{1}{2}, j_y + \tfrac{1}{2}) \\ &\times [\tilde{b}_{\nu-1,\mu}^{n+1}(j_x + \tfrac{1}{2}, j_y + \tfrac{1}{2}) + \delta_{1\nu}\delta_{0\mu}]. \end{aligned} \tag{36}$$

The indices j_x and j_y indicate that the quantities are to be taken at the position $x = j_x\,\Delta x$ and $y = j_y\,\Delta y$. The superscript n indicates that the quantity is calculated at a time $t = n\,\Delta t$. The tilde over a quantity ($\tilde{b}$) indicated that the quantity is to be approximated as follows.

$$\begin{aligned} \tilde{b}_{\nu,\mu}^{n+(1/2)}(j_x, j_y) = \tfrac{1}{4}[&b_{\nu,\mu}^{n+(1/2)}(j_x + \tfrac{1}{2}, j_y + \tfrac{1}{2}) + b_{\nu,\mu}^{n+(1/2)}(j_x + \tfrac{1}{2}, j_y - \tfrac{1}{2}) \\ &+ b_{\nu,\mu}^{n+(1/2)}(j_x - \tfrac{1}{2}, j_y + \tfrac{1}{2}) + b_{\nu,\mu}^{n+(1/2)}(j_x - \tfrac{1}{2}, j_y - \tfrac{1}{2})]. \end{aligned} \tag{37}$$

The values of $b_{\nu,\mu}$ calculated in Eqs. (35) and (36) are next used to integrate Eq. (34) in the y direction. Equation (34) is similar to Eq. (33); with the appropriate substitution of the indices ν and μ and the appropriate substitution of the dimension

y for x, one can write for Eq. (34) a difference scheme similar to the one in Eq.(35) and (36).

The electric field is calculated by solving Poisson's equation for the potential ϕ; at integer time-steps $t = n\,\Delta t$, and positions $x = j_x\,\Delta x$ and $y = j_y\,\Delta y$, we have

$$\nabla^2\phi\,\Big]^n_{j_x,j_y} = -b_{0,0}(j_x, j_y). \tag{38}$$

Equation (38) is solved for periodic boundary conditions using a fast Fourier transform algorithm. A similar equation that holds at half integer time-steps is obtained by substituting for n, j_x, and j_y in Eq. (38), by $n + \frac{1}{2}$, $j_x + \frac{1}{2}$, $j_y + \frac{1}{2}$, respectively. This leads to the value of the potential $\phi^{n+(1/2)}(j_x + \frac{1}{2}, j_y + \frac{1}{2})$. The electric field is calculated next from the potential by Fourier transforming the equation $\mathbf{E} = -\nabla\phi$. The integration of Eq. (35) at integer time-steps, however, necessitates prior knowledge of the electric field $E_x^{n+(1/2)}(j_x, j_y)$; because of this the value of the potential $\phi^{n+(1/2)}(j_x, j_y)$ has to be interpolated from that available for half integer time-steps $\phi^{n+(1/2)}(j_x + \frac{1}{2}, j_y + \frac{1}{2})$. This operation is effected using the fast Fourier transform algorithm to calculate the Fourier transform of the potential at a position shifted by $(\frac{1}{2}\,\Delta x, \frac{1}{2}\,\Delta y)$. The Fourier modes E_{xk} of E_x are then calculated and transformed back to obtain $E_x^{n+(1/2)}(j_x, j_y)$. A similar procedure is carried out for the integration at half time-steps in Eq. (36), where, in order to calculate $E_x^{n+1}(j_x + \frac{1}{2}, j_y + \frac{1}{2})$, the value of the potential at $\phi^{n+1}(j_x + \frac{1}{2}, j_y + \frac{1}{2})$ has to be interpolated from the value available for integer time-steps $\phi^{n+1}(j_x, j_y)$. The conservation properties and the stability of the leap-frog scheme have been discussed in detail in [5].

To include, in Eqs. (35) and (36), the damping term given in Eq. (32), we split this operator and use the damping operator

$$-(\nu + \mu)^{2r+1}(\lambda_x + \eta(\partial^2/\partial x^2))\, b_{\nu,\mu}(x, y, t) \tag{39}$$

for the integration in the x direction, and the damping operator

$$-(\nu + \mu)^{2r+1}(\lambda_y + \eta(\partial^2/\partial y^2))\, b_{\nu,\mu}(x, y, t) \tag{40}$$

for the integration in the y direction (with $\lambda = \lambda_x + \lambda_y$). A Dufort–Frankel scheme has been used for the diffusion operators $\partial^2/\partial x^2$ and $\partial^2/\partial y^2$ in order to increase the stability of the system [7, 12].

6. The Initialization of the Leapfrog Scheme

The leapfrog scheme expressed in Eqs. (35), (36) is a two-level scheme and must be initialized properly. For so doing, we followed the same steps as for the one-dimensional problem [5, 7] and used a two-level Lax–Wendroff scheme for the

initialization. We have followed the method of Gourlay and Morris [15] in constructing a two-dimensional, two-level Lax–Wendroff scheme which accomplished an initialization of second order in the time-step Δt. The initial value was integrated first in the x direction, then next in the y direction; the same initial value was taken back and integrated first in the y direction, then next in the x direction. The final integrated value has been taken as the average of the two previously integrated values. Details on this scheme can be found in [15].

As was pointed out by Knorr [5], the leapfrog scheme contains a parasitic mode of propagation which is not damped, and causes the two-levels of the scheme to drift apart. This difficulty was overcome in [5] by reinitializing the leapfrog scheme, after a number of time steps, before the drifting of the two levels became apparent. The same idea was applied in our present calculations; the Lax–Wendroff scheme, which was used for the initialization of the leapfrog scheme, has also been used to reinitialize the leapfrog scheme after each 20 time-steps.

7. Numerical Results

A. *The Free Streaming Case*

We first present the results obtained when the electric field is omitted in the Vlasov equation. We consider the initial value for the distribution function f at $t = 0$:

$$f(x, y, v_x, v_y, 0) = (1/2\pi) \exp(-\tfrac{1}{2}v_x^2 - \tfrac{1}{2}v_y^2)(A_x \cos k_x x + A_y \cos k_y y). \quad (41)$$

The substitution from Eq. (41) in Eq. (3) leads to

$$b_{0,0}(x, y, 0) = A_x \cos k_x x + A_y \cos k_y y, \quad (42)$$

$$b_{\nu,\mu}(x, y, 0) = 0 \qquad \nu, \mu \neq 0. \quad (43)$$

We calculate $f(x, y, v_x, v_y, t)$ from Eq. (13) and substitute in Eq. (3). After some straightforward algebra one finds that the time evolution of $b_{0,0}$ is given by

$$b_{0,0}(x, y, t) = \exp(-k_0^2 t^2/2)(A_x \cos k_0 x + A_y \cos k_0 y), \quad (44)$$

where it is assumed for simplicity that $k_x = k_y = k_0 = 2\pi/L$ (L is the length of the periodic system in both directions). Equation (44) indicates that the quantity $b_{0,0}(x, y, 0)$ given in Eq. (42) should decay exponentially in time as $\exp(-k_0^2 t^2/2)$. In Fig. 1, we have plotted the logarithm of the numerical values obtained for $b_{0,0}(L/4, 0)$, calculated with a matrix of $N_x = N_y = 15$ polynomials, $L = 2\pi$, $k_x = k_y = 1$, $A_x = A_y = 0.1$, using a time-step of $\Delta t = 1/16$ and a mesh of 16×16 points (curve (b)); we have also plotted the logarithm of the theoretical value of $b_{0,0}(L/4, 0)$, calculated from Eq. (44) (curve (a)). Figure 1 shows a very

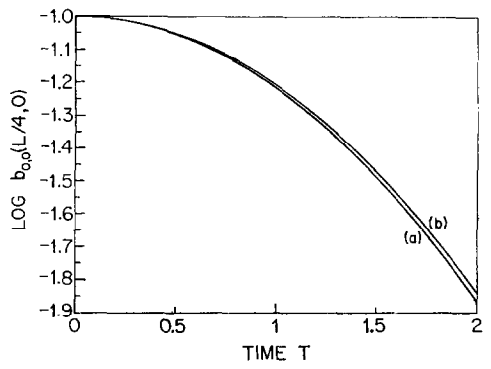

FIG. 1. Plot of the logarithm of the numerical value calculated for $b_{0,0}(L/4, 0)$, (curve (b)), together with the logarithm of the theoretical value taken from Eq. (44) (curve (a)) (for $N_x = N_y = 15$ polynomials, $k_x = k_y = 1.0$, $A_x = A_y = 0.1$, and $\Delta t = 1/16$).

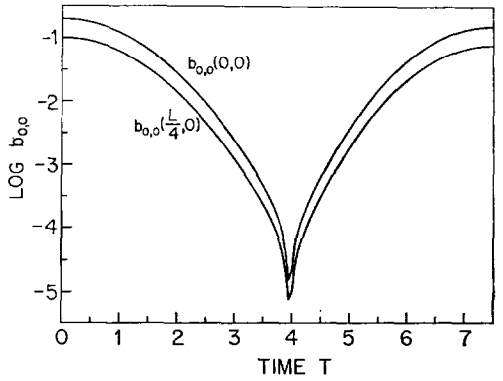

FIG. 2. Plot of the logarithm of the numerical value of $b_{0,0}(0, 0)$ and $b_{0,0}(L/4, 0)$ (using the same parameters as in Fig. 1, together with a small damping $\eta = (2 \times 13)^{-3}$, $\lambda_x = \lambda_y = (2 \times 13)^{-3}$, and $r = 1$).

good agreement between the theoretical and the numerical curves. Moreover a numerical curve obtained with a time-step $\Delta t = 1/32$ was found to coincide exactly with the theoretical curve (a). Figure 2 shows the logarithm of the value obtained for $b_{0,0}(0, 0)$ and $b_{0,0}(L/4, 0)$, up to a time $t = 7.5$ using a mesh of 8×8 points, the other parameters remaining the same as before. The results in Fig. 2, which were calculated using a very small damping $\eta = (2 \times 13)^{-3}$, $\lambda_x = \lambda_y = (2 \times 13)^{-3}$ and $r = 1$, show the expected parabolic decay followed by the recurrence effect. For the present parameters, the recurrence time calculated from Eq. (A.9) is $T_r = 7.74$. This value can be easily verified in Fig. 3, where the calculations have

been done with $\eta = 5(2 \times 13)^{-3}$, $\lambda_x = \lambda_y = 7.5(2 \times 13)^{-3}$ and $r = 1$. As can be seen in Fig. 3, the values of $b_{0,0}(0, 0)$ and $b_{0,0}(L/4, 0)$ at recurrence time have been reduced to about 3 % of their original values.

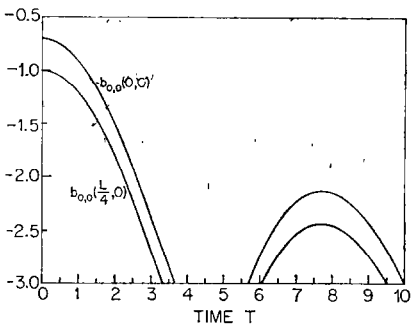

FIG. 3. Same as in Fig. 2, but the damping has been increased to $\eta = 5.0\ (2 \times 13)^{-3}$, $\lambda_x = \lambda_y = 7.5\ (2 \times 13)^{-3}$ and $r = 1$. The amplitude at recurrence is reduced to about 3 % of its original value.

If one chooses, as initial condition, the distribution

$$f(x, y, v_x, v_y, 0) = (1/2\pi) \exp(-\tfrac{1}{2}v_x^2 - \tfrac{1}{2}v_y^2)(1 + A_x \cos k_0 x + A_y \cos k_0 y), \tag{45}$$

then the substitution from Eq. (45) in Eq. (3) leads to

$$b_{0,0}(x, y, 0) = 1 + A_x \cos k_0 x + A_y \cos k_0 y. \tag{46}$$

The time evolution of f is given by Eq. (13), which, together with Eq. (3), leads to

$$b_{0,0}(x, y, t) = 1 + \exp(-k_0^2 t^2/2)(A_x \cos k_0 x + A_y \cos k_0 y). \tag{47}$$

Equation (47) shows that $b_{0,0} \to 1$ as $t \to \infty$. In Fig. 4a we have plotted the logarithm of the numerical value calculated for $b_{0,0}(0, L/4)$ (curve (b)), together with the logarithm of the theoretical value calculated from Eq. (47) (curve (a)). The parameters used are $A_x = A_y = 0.1$, $k_x = k_y = k_0 = 1\ (L = 2\pi)$; $N_x = N_y = 15$ polynomials, a mesh of 8×8 points, and a time step $\Delta t = 1/16$. Figure 4a shows a very good agreement between the theoretical and the calculated curve, until the recurrence effect becomes apparent. (In this case, the recurrence effect causes the initial curve to reappear upside down.) Figure 4b shows a plot of the logarithm of the numerical values calculated for $b_{0,0}(0, 0)$ and $b_{0,0}(L/4, 0)$. The results in Fig. 4 were calculated by adding too small a damping ($\eta = (2 \times 13)^{-3}$, $\lambda_x = \lambda_y = (2 \times 13)^{-3}$, $r = 1$) and, as can be seen, the recurrence effect remains important.

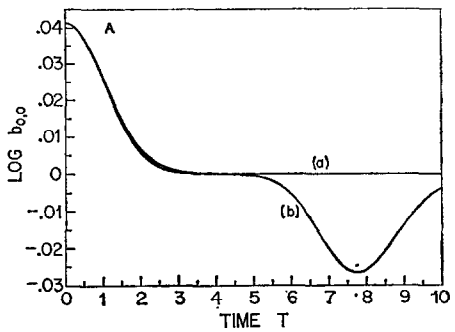

FIG. 4a. Plot of the logarithm of the numerical value calculated for $b_{0,0}(0, L/4)$, (curve (b)), together with the theoretical value derived from Eq. (47). (For $N_x = N_y = 15$ polynomials, $k_x = k_y = 1.0$, $A_x = A_y = 0.1$, and $\Delta t = 1/16$ and a small damping $\eta = \lambda_x = \lambda_y = (2 \times 13)^{-3}$, $r = 1$).

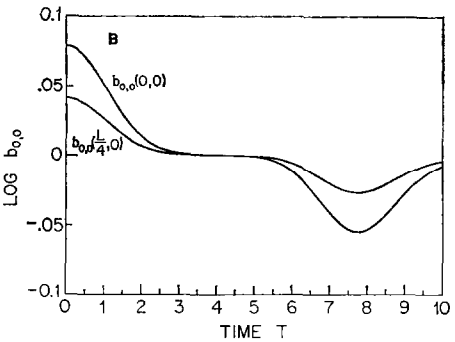

FIG. 4b. Plot of the logarithm of the numerical value of $b_{0,0}(0, 0)$ and $b_{0,0}(L/4, 0)$ (using same parameters as in Fig. (4a)).

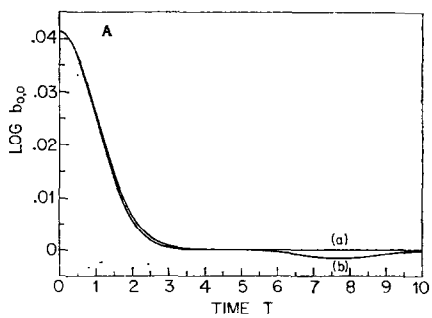

FIG. 5a. Same as in Fig. 4a, but the damping has been increased to $\eta = 5.0(2 \times 13)^{-3}$ and $\lambda_x = \lambda_y = 7.5(2 \times 13)^{-3}$. The recurrence effect has been almost completely eliminated.

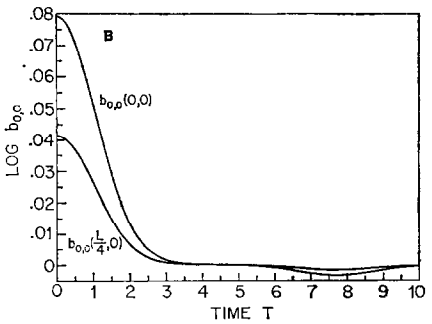

FIG. 5b. Same as in Fig. 4b, but the damping has been increased to $\eta = 5.0(2 \times 13)^{-3}$ and $\lambda_x = \lambda_y = 7.5(2 \times 13)^{-3}$. The recurrence effect has been almost completely eliminated.

In Figs. 5a, and b, we have repeated the same calculations as in Figs. 4a, and b but, this time, using a larger damping ($\eta = 5(2 \times 13)^{-3}$, $\lambda_x = \lambda_y = 7.5(2 \times 13)^{-3}$). As can be seen, the recurrence effect is almost completely eliminated, the numerical curves remain very close to the asymptotic value of 1 indicated by Eq. (47). From Eq. (A.9) the value of the recurrence time is found to be $T_R = 7.74$; this value is in very good agreement to that which can be inferred from Figs. 4 and 5.

B. *The Linear Landau Damping*

We have linearized Eqs. (1) and (2) around an equilibrium f_0 by assuming

$$f = f_0 + f_1, \qquad f_1 \ll f_0 \tag{48}$$

and have chosen for f_0 the Maxwellian distribution given in Eq. (9). Also, we have chosen for f_1, at $t = 0$, a perturbation of the form

$$f_1(x, y, v_x, v_y, 0) = f_0\, g(x, y), \tag{49}$$

where f_0 is defined in Eq. (9), and $g(x, y)$ will be given different values to be discussed later on. The expansion of $f_1(x, y, v_x, v_y, t)$, using the series given in Eq. (3), together with the linearization of the Vlasov equation, leads to an equation which is identical to Eq. (10), where the terms $E_x b_{\nu-1,\mu}$ and $E_y b_{\nu,\mu-1}$ are omitted and the electric field appear only through the terms $E_x \delta_{1\nu}\delta_{0\mu}$ and $E_y \delta_{0\nu}\delta_{1\mu}$. Analytic solutions for the linearized two-dimensional Vlasov equation are available in the literature for the Maxwellian equilibrium distribution [16, 17]. Several cases with different values of $g(x, y)$ will be considered here.

1. $E_x \neq 0$, $E_y = 0$. We consider first the case when $g(x, y)$ is function of x only

$$g(x, y) = A_x \cos k_x x, \tag{50}$$

where we have taken $A_x = 0.05$, $k_x = k_y = 1$ ($L = 2\pi$). In this case, the Fourier component $E_{xk}(1, 0)$ of the electric field E_x is present at $t = 0$ and will decay exponentially in time according to the theory of Landau damping. The field component $E_y = 0$ at $t = 0$ and remains zero for all time t. Figure 6 shows the exponential decay of E_{xk} plotted on a logarithmic scale against time. The numerical values for ω/ω_p (frequency of the oscillation) and γ/ω_p (damping rate of the oscillation) are 1.95 and 0.88, respectively, while the corresponding theoretical values are 2.046 and 0.851 [17]. The agreement can be considered as being very good, especially if one keeps in mind that we are using a mesh of 8×8 points only. We are also using a matrix of $N_x = N_y = 40$ polynomials, and a time-step $\Delta T = 1/16$; no damping is used in these calculations ($\eta = \lambda_x = \lambda_y = 0$). In this case Eq. (A.9) indicates a recurrence time $T_R = 12.64$ (the beginning of the recurrence effect is apparent at the end of Fig. 6).

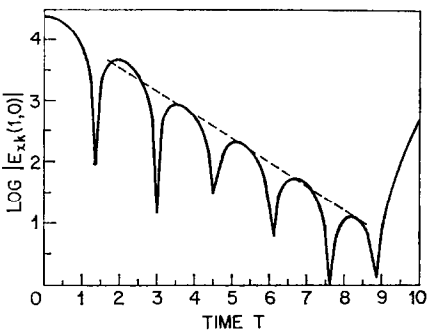

FIG. 6. Linear Landau damping calculated from the linearized equation for parameters given in cases B1 and B2.

2. *The presence of two modes* $E_{xk}(1, 0)$ *and* $E_{yk}(0, 1)$. We consider next the case when $g(x, y)$ is given by

$$g(x, y) = A_x \cos k_x x + A_y \cos k_y y. \tag{51}$$

We choose $A_x = A_y = 0.05$, $k_x = k_y = 1$ ($L = 2\pi$). At $t = 0$, the Fourier components for E_x and E_y are, respectively, $E_{xk}(1, 0)$ and $E_{yk}(0, 1)$. One can look for a solution of the linearized Vlasov equation of the form

$$f_1(x, y, v_x, v_y, t) = f_{1x}(x, v_x, v_y, t) + f_{1y}(y, v_x, v_y, t), \tag{52}$$

where

$$f_{1x}|_{t=0} = f_0 A_x \cos k_x x, \tag{53}$$

$$f_{1y}|_{t=0} = f_0 A_y \cos k_y y. \tag{54}$$

In this case the linearized Vlasov equation can be written as

$$\frac{\partial}{\partial t}(f_{1x}+f_{1y})+v_x\frac{\partial f_{1x}}{\partial x}+v_y\frac{\partial f_{1y}}{\partial y}+E_x\frac{\partial f_0}{\partial v_x}+E_y\frac{\partial f_0}{\partial v_y}=0, \tag{55}$$

which can be split into

$$(\partial f_{1x}/\partial t)+v_x(\partial f_{1x}/\partial x)+E_x(\partial f_0/\partial v_x)=0, \tag{56}$$

$$(\partial f_{1y}/\partial t)+v_y(\partial f_{1y}/\partial y)+E_y(\partial f_0/\partial v_y)=0. \tag{57}$$

This means that the solution of the linearized two-dimensional Vlasov equation is the sum of the two solutions obtained from the two one-dimensional equations (Eqs. (56) and (57)). This fact is verified exactly by the numerical scheme, where the Fourier components $E_{xk}(1, 0)$ and $E_{yk}(0, 1)$ are found to remain exatly equal in time, decaying with the same damping rate and oscillating with the same frequency. Furthermore, since Eqs. (56) and (57) are equivalent to the equation one gets for case (1) when $E_y = 0$, and since we are using identical initial conditions in Eqs. (53) and (55) as in Eq. (50), it follows that the curves one gets in the present case are identical to the curve (Fig. 6) one gets for case (1). This identity has been verified exactly by the numerical scheme.

3. *The presence of two modes* $E_{xk}(0.5, 0.5)$ *and* $E_{yk}(0.5, 0.5)$. We consider now the case when $g(x, y)$ is given by

$$g(x, y) = A_x \cos k_x x \cos k_y y. \tag{58}$$

We choose $A_x = 0.05$, $k_x = k_y = 0.5$ ($L = 4\pi$). The electric field components E_x and E_y have, at $t = 0$, the Fourier components $E_{xk}(0.5, 0.5)$ and $E_{yk}(0.5, 0.5)$, respectively. These components are equal at $t = 0$ and remain equal for all time t.

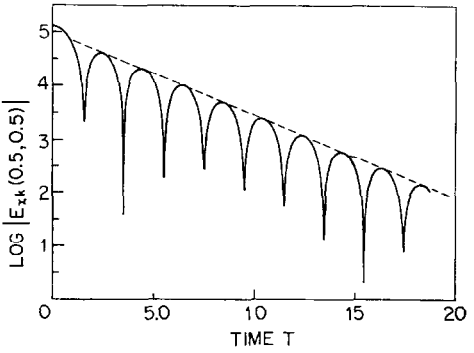

FIG. 7. Linear Landau damping calculated from the linearized equation for parameters given in case B3.

Figure 7 shows the exponential decay of E_{xk} plotted on a logarithmic scale against time (E_{yk} gives an identical curve). The numerical values for ω/ω_p and γ/ω_p are 1.58 and 0.35 respectively, while the theoretical values for $k = (k_x^2 + k_y^2)^{1/2} = 0.707$ are 1.67 and 0.39, respectively [17]. The agreement is considered very good, bearing in mind that we are using a mesh of 8 × 8 points only. We have used a matrix of $N_x = N_y = 40$ polynomials and a time-step of $\Delta T = 1/16$. No damping has been added in this case ($\eta = \lambda_x = \lambda_y = 0$). (From Eq. (A.9) the recurrence time is $T = 25.0$). The calculations have been carried up to $t = 18.75$ and have

4. *Solution of the nonlinear Vlasov equation.* As a further check of our fortran code, we have solved the full nonlinear Vlasov equation under the same initial conditions as in Section B2, but with $k_x = k_y = 0.5$ ($L = 4\pi$). The calculations have been done up to $t = 10$, with a mesh of 16 × 16 points, to allow for an adequate representation of the higher harmonics; we have also used 30 × 30 polynomials. These calculations required almost four hours using an IBM 370/168. One expects the two modes $E_{xk}(0.5, 0)$ and $E_{yk}(0, 0.5)$ to damp linearly at the early evolution of the system. The results are shown in Fig. 8. In Fig. 8a, the fundamental mode $E_{xk}(0.5, 0)$ is decaying linearly according to the Landau theory (the calculated values are $\omega/\omega_p = 1.48$ and $\gamma/\omega_p = 0.158$, to be compared with the theoretical values of $\omega/\omega_p = 1.415$ and $\gamma/\omega_p = 0.1533$); the mode $E_{yk}(0, 0.5)$ remained exactly equal to $E_{xk}(0.5, 0)$, decaying with the same damping rate. Furthermore, the excited harmonics of E_{xk} and E_{yk} were also exactly equal. Figures 8b and 8c show the higher modes $E_{xk}(1, 0)$ and $E_{xk}(0.5, 0.5)$; their amplitude remained at least two orders of magnitude less than the amplitude of the fundamental E_{xk} mode. The modes $E_{yk}(0, 1)$ and $E_{yk}(0.5, 0.5)$ remained exactly equal to $E_{xk}(1, 0)$ and $E_{xk}(0.5, 0.5)$, respectively. Hence, most of the electric energy remained in the

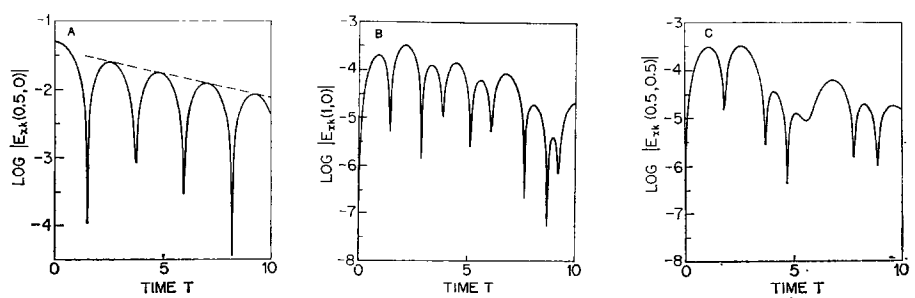

FIG. 8. (a) Linear Landau damping for the fundamental $E_{xk}(0.5, 0)$ mode obtained by solving the full nonlinear equation as discussed in case B4. (b) The harmonic $E_{xk}(1, 0)$ excited when solving the full nonlinear Vlasov equation as discussed in case B4. (c) The harmonic $E_{xk}(0.5, 0.5)$ excited when solving the full nonlinear Vlasov equation as discussed in case B4.

fundamental mode. Figure 9 shows, on a linear scale, the exponential decay of the total electric energy.

These calculations were done with a time-step $\Delta T = 1/16$; at $t = 10$ (i.e., after 160 iterations) the relative error in the total energy was 1.48×10^{-4}.

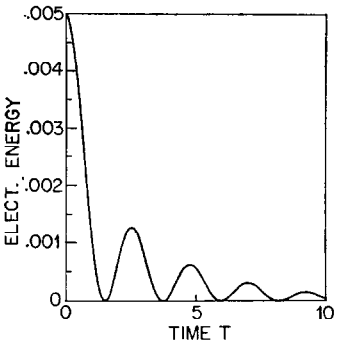

FIG. 9. Exponential decay of the electric energy, plotted on a linear scale, for the case discussed in B4 when solving the full nonlinear equation.

8. CONCLUSION

In the present work, we have developed a numerical scheme for the solution of a two dimensional Vlasov equation. The equation is first transformed in velocity space by expanding the distribution function in terms of Hermite polynomials, and then a multistep technique is used which consists in splitting up the transformed two dimensional equations and integrating it alternatively in each dimension in the configuration space. The results for the free streaming case and the linear Landau damping, which have been discussed in Section 7, show a very good agreement with the theory.

The present results (with the exception of Section (B4) have been obtained using the IBM 370/155 of Laval University. The results for the linear Landau damping in Figs. 6 and 7 have been obtained using a matrix of 40×40 polynomials and a mesh of 8×8 points, with a time step $\Delta T = 1/16$; this has been effected without applying any damping to the finite matrix to eliminate the recurrence effect, in order to test the correctness of the scheme and to get a good comparison with available analytical results. The results presented in Figs. 8 and 9 have been obtained using the full nonlinear equation with a matrix of 30×30 polynomials and a mesh of 16×16 points; our fortran program required in this case almost 4 hours of calculation using the IBM 370/168 of the Ministry of Education of the Provincial Government of Quebec. These results, calculated up to $t = 10$, show

a linear behavior dominating at the early evolution of the sytem, as one would expect under the initial conditions used in Section B4. The results in Figs. 8 and 9 could have been easily obtained using a mesh of 8×8 points and a matrix of only 10×10 polynomials. This was not done, however, because it was desired to know the computation time required for calculations performed with the same sets of matrices as we plan to use when carrying out simulations of nonlinear effects using the present 2-D code.

In the present work, priority has been given to testing the correctness of the numerical scheme, the economy in the computational effort being of less immediate importance. The addition of damping should effectively eliminate the recurrence effect (as it has been successfully verified for the free streaming case in Figs. 3 and 5), and should make it possible to reduce the number of polynomials used in the simulation. The optimized code should make it possible to simulate nonlinear effects with a matrix of 30×30 polynomials and a mesh of 16×16 points, i.e., the equivalent of $(480)^2$ "particles"; this is equivalent to the simulation of a one-dimensional nonlinear Vlasov equation with 480 "particles," which is the optimized result reported for the one-dimensional case in [5, 7, 8].

APPENDIX: Estimation of the Recurrence Time for the Truncated Matrix

In order to estimate the recurrence time for the truncated matrix, we first consider the continuous spectrum of the infinite matrix for the free streaming case. The eigenvalues ω_x and ω_y defined in Eq. (20) are continuous. Because of the linearity of the system, one can write the general solution of the system as a superposition of elementary solutions; from Eqs. (3) and (15)–(23) we get

$$f(x, y, v_x, v_y, t) = \frac{1}{2\pi} \sum_{\nu=0}^{\infty} \sum_{\mu=0}^{\infty} \frac{H_{e\nu}(v_x)}{\nu!} \frac{H_{e\mu}(v_y)}{\mu!} \exp(-\tfrac{1}{2}v_x^2 - \tfrac{1}{2}v_y^2) \exp(ik_x x + ik_y y)$$

$$\cdot \int_{-\infty}^{\infty} \int_{-\infty}^{\infty} A(S_x, S_y)\, H_{e\nu}(S_x)\, H_{e\mu}(S_y) \exp(ik_x S_x t + ik_t S_y t)\, dS_x\, dS_y, \tag{A.1}$$

where we have set $S_x = \omega_x/k_x$, $S_y = \omega_y/k_y$, and where the coefficient $A(S_x, S_y)$ is to be determined from the initial condition.

Assume (as we did in our calculations) an initial perturbation of the form

$$f(x, y, v_x, v_y, 0) = (1/2\pi) \exp(-\tfrac{1}{2}v_x^2 - \tfrac{1}{2}v_y^2) \exp(ik_x x + ik_y y). \tag{A.2}$$

Substituting from Eq. (A.2) in Eq. (A.1) for $t = 0$, one can readily verify that a solution for $A(S_x, S_y)$ in this case is given by

$$A(S_x, S_y) = (1/2\pi) \exp(-\tfrac{1}{2}S_x^2 - \tfrac{1}{2}S_y^2). \tag{A.3}$$

We substitute from Eq. (A.3) in Eq. (A.1); to evaluate the integral in Eq. (A.1), we use the generating function for the Hermite polynomials:

$$e^{SZ-(1/2)Z^2} = \sum_{n=0}^{\infty} (1/n!)\, H_{en}(S)\, Z^n. \tag{A.4}$$

Equation (A.4), together with the orghogonality relation for the Hermite polynomials, leads to

$$\int_{-\infty}^{\infty} H_{e\mu}(S)\, e^{SZ-(1/2)Z^2} e^{-(1/2)S^2}\, dS = (2\pi)^{1/2}\, Z^{\mu}. \tag{A.5}$$

Hence we have obtained the result

$$\int_{-\infty}^{\infty} H_{e\mu}(S)\, e^{SZ-(S^2/2)}\, dS = (2\pi)^{1/2}\, Z^{\mu} e^{(1/2)Z^2}. \tag{A.6}$$

Substituting in Eq. (A.6) successively by $S = S_x$ and $Z = ik_x t$, $S = S_y$ and $Z = ik_y t$, we get for f, from Eq. (A.1):

$$f(x, y, v_x, v_y, t) = \frac{1}{2\pi} \sum_{\nu=0}^{\infty} \sum_{\mu=0}^{\infty} (ik_x t)^{\nu} (ik_y t)^{\mu} \exp(-\tfrac{1}{2}(k_x^2 + k_y^2)\, t^2)$$
$$\cdot \frac{H_{e\nu}(v_x)}{\nu!} \frac{H_{e\mu}(v_y)}{\mu!} \exp(-\tfrac{1}{2}v_x^2 - \tfrac{1}{2}v_y^2) \exp(ik_x x + ik_y y). \tag{A.7}$$

Equation (30) indicates a time behavior for the ν, μ mode proportional to $t^{\nu+\mu} \exp(-\frac{1}{2}(k_x^2 + k_y^2)\, t^2)$. Extending to the two dimensions the formalism used by Knorr [5] in one dimension one can picture the perturbation which starts for $t = 0$ at $b_{0,0}$ (given in Eq. (42) or (46)), as a signal with starts for $t = 0$ at $\nu = \mu = 0$ and then propagates to higher values of (ν, μ). From Eq. (A.7), the signal will reach the mode ν, μ at the time when the quantity $t^{\nu+\mu} \exp(-\frac{1}{2}(k_x^2 + k_y^2)\, t^2)$ is maximum, i.e., at a time t given by

$$t = (\nu + \mu)^{(1/2)}/(k_x^2 + k_y^2)^{(1/2)}. \tag{A.8}$$

An estimation of the recurrence time for a truncated matrix can be obtained as follows. If the infinite matrix is truncated at, say, $\nu = N_x$, and $\mu = N_y$, the time it takes for a perturbation to reach the boundary of the truncated matrix at the "mode" (N_x, N_y) can be calculated from Eq. (A.8); if we estimate that it takes an equal time for the perturbation to return back to the origin, one can get for the recurrence time the estimation

$$T_R = 2((N_x + N_y)^{(1/2)}/(k_x^2 + k_y^2)^{(1/2)}). \tag{A.9}$$

For $N_x = N_y = 15$ and $k_x = k_y = 1$, we get $T_R = 7.74$, a value which is in excellent agreement with the numerical results given in Figs. 3, 4, and 5.

ACKNOWLEDGMENTS

The authors are grateful to the Computer Center staff at Laval University for much assistance, especially by M. R. Miville-Dechesnes and J.-M. Lavoie. The authors are also grateful to the authorities of the "Direction Générale de l'Enseignement Supérieur," for special permission to use the IBM 370/168 of the Ministry of Education of the Provincial Government of Quebec (SIMEQ), as well as to the SIMEQ authorities, who made it possible to obtain the curves given in Figs. 8 and 9. The constant interest and encouragement of M. M. Lecours, head of Electrical Engineering Department, is gratefully acknowledged. M. Shoucri is grateful to Professor G. Knorr for many discussions, and for many of the ideas developed in the present work.

REFERENCES

1. T. ARMSTRONG, R. HARDING, G. KNORR, AND D. MONTGOMERY, *in* "Methods in Computational Physics," Vol. 9, p. 70, Academic Press, New York, 1969.
2. G. JOYCE, G. KNORR, AND H. MEIER, *J. Computational Phys.* **8** (1971), 53.
3. F. G. GRANT AND M. FEIX, *Phys. Fluids* **10** (1967), 1356.
4. T. ARMSTRONG, *Phys. Fluids* **10** (1967), 1269.
5. G. KNORR, *J. Computational Phys.* **13** (1973), 165.
6. J. NÜEHRENBERG, *Z. Angew. Math. Phys.* **22** (1971), 1057.
7. M. SHOUCRI AND G. KNORR, *J. Computational Phys.* **14** (1974), 84.
8. M. SHOUCRI AND R. R. J. GAGNÉ, *J. Computational Phys.* **21** (1976), 238.
9. C.-Z. CHENG AND G. KNORR, "The Integration of the Vlasov Equation in Configuration Space," Univ. of Iowa, Rept. No. 75–24, 1975.
10. J. DENAVIT, Numerical solution of the Vlasov equation, *in* "Proceedings of the Fourth Conference on Numerical Simulation of Plasmas" (J. Boris and A. Shanny, Eds.), Naval Research Lab., Washington, D. C., 1970.
11. N. N. YANENKO, "The Method of Fractional Steps," Springer–Verlag, New York, 1971.
12. M. M. SHOUCRI AND R. R. J. GAGNÉ, *Bull. Amer. Phys. Soc.* **20** (1974), 1368.
13. J. CANOSA, J. GAZDAG, AND J. E. FROMM, *J. Computational Phys.* **15** (1974), 34.
14. G. KNORR AND M. SHOUCRI, *J. Computational Phys.* **14** (1974), 1.
15. A. R. GOURLAY AND J. L. MORRIS, *Math. Comp.* **22** (1968), 715.
16. D. MONTGOMERY, "Theory of the Unmagnetized Plasma," Gordon and Breach, New York, 1971.
17. J. CANOSA, *J. Computational Phys.* **13** (1973), 158.